HHS Public Access

Author manuscript

Gene Ther. Author manuscript; available in PMC 2016 May 18.

Published in final edited form as:

Gene Ther. 2016 February ; 23(2): 151–157. doi:10.1038/gt.2015.100.

Liquid Jet Delivery Method Featuring S100A1 Gene Therapy in the Rodent Model Following Acute Myocardial Infarction

Anthony S. Fargnoli, PhD[1], **Michael G. Katz, MD, PhD**[1], **Richard D. Williams, BS**[1], **Andrew P. Kendle, BS**[1], **Nury Steuerwald, PhD**[2], and **Charles R. Bridges, MD, ScD**[1]

[1]Department of Thoracic and Cardiac Surgery, Sanger Heart & Vascular Institute, Carolinas HealthCare System, Charlotte, North Carolina

[2]Molecular Biology Core, Cannon Research Center, Carolinas HealthCare System, Charlotte, North Carolina

Abstract

The S100A1 gene is a promising target enhancing contractility and survival post myocardial infarction (MI). Achieving sufficient gene delivery within safety limits is a major translational problem. This proof of concept study evaluates viral-mediated S100A1 overexpression featuring a novel liquid jet delivery (LJ) method. 24 rats after successful MI were divided into 3 groups (n=8 ea.): saline control (SA), ssAAV9.S100A1 (SS) delivery, and scAAV9.S100A1 (SC) delivery (both 1.2×10^{11} viral particles). For each post MI rat, the LJ device fired three separate 100 μL injections into the myocardium. Following 10 weeks, all rats were evaluated with echocardiography, quantitative polymerase chain reaction (qPCR), and overall S100A1 and CD38 immune protein. At 10 weeks all groups demonstrated a functional decline from baseline, but the S100A1 therapy groups displayed preserved LV function with significantly higher ejection fraction %; SS group [60±3] and SC group [57±4] versus saline [46±3], $p<0.05$. Heart qPCR testing showed robust S100A1 in the SS [10,147±3993] and SC [35,155±5808] copies per 100 ng DNA, while off target liver detection was lower in both SS [40±40], SC [34,841±3164] respectively. Cardiac S100A1 protein expression was [4.3±0.2] and [6.1±0.3] fold higher than controls in the SS and SC groups respectively, $p<0.05$.

Introduction

The S100A1 gene is a promising target enhancing contractility, energetics and myocyte survival post myocardial infarction (MI)[1,2]. This potent target is rapidly approaching clinical trials, with the unique ability to restore critical Ca^{2+} cycling mechanisms perturbed in heart failure[3]. Recent evidence suggests S100A1 may have a significant advantage over other targets, since it has a key role in both maintaining myofibril integrity and regeneration[4–6].

Address correspondence to: Dr. Anthony Fargnoli, Sanger Heart and Vascular Institute, 1542 Garden Terrace, Charlotte, NC28203; ; Email: Anthony.Fargnoli@carolinashealthcare.org; phone: (704) 355-5902; fax: (704) 355-7202

No conflicts of interest, financial or otherwise, are declared by the authors.

Disclosures: No conflicts of interest, financial or otherwise, are declared by the authors.

Despite this level of interest in S100A1, achieving sufficient myocardial delivery within safety limits is a major translational problem. Although there are very positive results presented in transgenic models[7,8] the relationships between: delivery route, vector selection, the resultant in vivo pharmacodynamics, and associated host response risks are not clearly established[9,10]. Sequential studies in larger species do not provide a quantitative relationship between the necessary transfer levels in the cardiac tissue counterbalanced by host response risks resulting - at least in part - from excessive off target expression[11]. It is now established that the level of cardiac transfer and collateral organ exposure results from a complex interaction of: target tissue disease level, route of administration, viral vector serotype, viral vector molecular design, and dose level[12].

The design of more efficient delivery routes (i.e. defined as achieving a greater % of transduction in myocytes versus collateral tissues per dose) of administration has advanced with numerous minimally invasive and surgical applications designed to maximize efficiency[12,13] The first cardiac gene therapy trial led by Rosengart *et al.* featured delivery via simple readily applicable intramuscular injection (IM) of adenovirus encoding vascular endothelial growth factor for angiogenesis[14]. Since then, the majority of AAV trials have employed percutaneous catheterization for infusion advocating a more homogenous transfer pattern from the primary infusion vessel. Yet, delivery problems still remain since very high doses are required for any detectable improvements in outcome[15–17].

In fact most recently the Calcium Up-Regulation by Percutaneous Administration of Gene Therapy in Cardiac Disease (CUPID2) trial failed to meet its primary endpoints using high doses via the intracoronary route. This reaffirms the importance of investigating new delivery technology to maximize efficiency while also considering the choice of vector/gene for the intended cardiovascular application. Our group has introduced the concept of applying a novel liquid jet methodology for cardiac gene therapy. This method depicted in (Figure 1A) seeks to provide direct delivery into myocardium via surgical window promoting maximal retention, yet disperse delivery per injection. The key working principle is that safe, maximal cardiac retention of vector therapeutic can be achieved with the careful adjustment of several key variables including: driving pressure, nozzle distance, and jet dispersion. Our previous work established the methodology and validated this approach in a rodent model[18], shown in (Figure 1B). The key finding in this study was that the liquid jet offered the same level of gene transfer as compared with aggressive occlusion infusion approaches, while at the same time having less collateral organ expression.

In parallel, advances in recombinant AAV vector design have improved vector transduction efficiency, achieving greater genome copy transfer while reducing the required number of vector particles (i.e. dose). This improvement in vector design thus in theory reduces the risk of immune complications secondary to excess off-target expression. One key innovation by Samulski *et al*[19–20] was the development of the self-complementary adeno-associated vector (scAAV), which avoids a key rate limiting DNA conversion step post cell entry[21,22]. Multiple studies have demonstrated the use of scAAV vector's advantage over ssAAV for a variety of muscle applications demonstrating a rapid onset of gene expression[23,24]. S100A1 is an excellent candidate for inclusion into a scAAV, since itscDNA has only300 base pairs, well within the cloning limit of scAAV (~ 3.3Kb)[25].

This study offers two unique investigative aims. One is to evaluate the potential of liquid jet mediated therapy as an effective route of AAV administration post MI. The second is to compare the therapeutic efficacy, genome copy biodistribution and degree of inflammatory stimulus associated with ssAAV and scAAV with liquid jet delivery. We assert that the methodology and results of this study can serve as a model for future pharmacodynamic assessments for cardiac gene therapy, in particular to carefully examine the risk/reward profile with a selected delivery method/vector/dose configuration.

Results

All animals with successful MI creation (24/30) were subjected to liquid jet delivery, recovered and survived without any complications to 10 weeks. There were 6 animals that were either euthanized or excluded from any particular delivery group due to variable anatomy or arrhythmia complications following the left anterior descending arterial ligation.

Echocardiography Data: S100A1's Impact on Structure and Function

The Saline (SA), single stranded AAV.S100A1 (SS) and self-complementary AAV.S100A1 (SC)groups all exhibited global remodeling parameters typical of post MI course at 10 weeks with significant increases in End Diastolic Volume Index [1.33±0.1, 1.22±0.2, 1.33±0.2 mL/cm^2], End Systolic Volume Index [0.73±0.1, 0.49±0.1, 0.57±0.2 mL/cm^2] and Left Ventricular Area [1.5±0.1, 1.4±0.2, 1.5±0.1 cm^2] from original respective baseline values {[0.71±0.1, 0.62±0.1, 0.76±0.04 mL/cm^2], [0.24±0.05, 0.19±0.03, 0.23±0.02 mL/cm^2] and [0.8±0.1, 0.7±0.1, 0.8±0.1 cm^2]} respectively as shown in Table 1, all $p<0.05$. The S100A1 gene therapy groups at 10 Weeks however had significantly preserved Ejection Fraction in SS [60±3%] and SC [57±4%] versus SA controls [46±3%], $p<0.05$, Figure 2A. This performance improvement in systolic function was also confirmed when comparing stroke volume index changes from baseline Table 1, with both treatment SS [0.30±0.04 mL/cm^2] and SC [0.25±0.05 mL/cm^2] demonstrating improvement in contrast to the SA [0.1±0.03 mL/cm^2], $p<0.01$. The gene therapy treatment groups also exhibited preserved myocardial baseline structure Table 1 as measured by average global wall thickness at 10 weeks both in the SS [1.5±0.1 mm] and SC [1.5±0.1 mm] while the SA [1.2±0.1 mm] deteriorated, $p<0.05$, Figure 2B.

Infarct Size Characterization

The Masson's trichrome infarct area detection revealed that all 3 groups had a variable, but non-significant difference in infarct scoring with the SA [29±4%], SS [25±4%], and SC [37±6%]. The primary affected myocardial zones defined in the analysis ranged from the anteroseptal to posterolateral wall regions.

qPCR Detection of AAV.S100A1 Genomes: Cardiac Specificity Level by Treatment Group

The SA control specimens yielded undetectable values serving as negative control and 10/96 samples analyzed were reported out of the range. All animals in both gene therapy groups exhibited high levels of detectable AAV. S100A1 the rapeutic copies. Quantification results indicated that there was a major discrepancy in myocardial transfer levels between SS and SC specimens, thus confirming the SC vector's superior transfection efficiency. The SC

group's cardiac levels were [35.2±5.8] compared with SS at [10.1±3.6] thousand S100A1 copies per 100 ng DNA, $p<0.05$. Likewise, but to a much greater proportion in the collateral liver specimens, a greater copy number amount was found in the SC [34.8±3.2] versus minimal detection in the SS [0.04±0.04] thousand S100A1 copies per 100 ng DNA, all $p<0.05$, Figure 3. Thus the SS group had greater cardiac specificity in terms of cardiac/liver transduction (e.g. 250:1) versus SC which was roughly 1:1.

Quantitative Immunofluorescence of Cardiac S100A1 and Immune Activator CD38

Robust myocardial overexpression of therapeutic S100A1 was found in the majority of cardiac regions confirming the dispersive delivery profile. Figure 4A demonstrates a typical cardiac SS specimen. On average, more robust S100A1 expression was found in the SC group as higher intensity detection is shown in Figure 4B. Figure 4C demonstrates average S100A1 levels in the SA group, which served as the normalization basis. The quantitative analysis confirmed these conclusions whereby the SS [4.3±0.1] and SC [6.1±0.3] both demonstrated higher S100A1 normalized to the SA controls [1.0±0.1], all $p<0.05$. Figure 5A. The CD38 results depicted in Figure 5B indicate that the SC exhibited dramatically higher levels [8.0.±0.3] as compared with the SS [3.8.±0.2].

AAV Mediated S100A1 Myocyte Transduction Efficiency

Additional detailed confocal analysis in the consistent peak expressing left ventricular anteriorlateral wall region revealed that liquid jet injection yielded consistently high myocyte S100A1 transduction efficiencies. The results were SS group [69±2%] and SC [71±3%], ns.

Discussion

Liquid jet injection technology when applied with an optimized velocity/dispersion profile achieved efficacious S100A1 overexpression in post MI rat myocardium with two different AAV vectors at the same dose level. These results in conjunction with those found in the latest large animal studies solidify S100A1's position as a promising heart failure target [26,27]. Our previous liquid jet methodology study argued that the advantage of this route's approach over intramuscular injection is that it facilitates AAV transfer through greater percentage of myocardial mass per injection due to its dispersive, higher retention profile[18]. This is the first proof of concept infarct study using liquid jet administration of AAV encoding a clinically relevant therapeutic transgene. The results essentially demonstrate functional improvement in systolic function in the setting of irreversible LV damage and subsequent remodeling course.

This study also offers several unique points with respect to translational considerations, specifically the difference in vector performance with the route and dose held constant. The first was the observation of the non-linearity with the corresponding qPCR detected AAV. S100A1 GC and realized post MI S100A1 overexpression at 10 weeks. The quantitative confocal S100A1 demonstrated that a range of 4 to 6 (i.e. SS to SC efficacy range) fold normalized to control group protein was sufficient to improve systolic function and maintain structural integrity post MI. The SC vector resulted in a 3.5 fold higher GC number in the

myocardium as compared with SS, but only resulted in 1.4× fold more S100A1 protein detection. Taken together these results suggest that the myocardium may reach a maximum transduction threshold, whereby additional GC presence is inconsequential past a saturation limit. This upper limit will most likely vary per delivery method; however it is essential to quantify the relationship for optimal vector/dose selection.

Following from the concept of an upper transduction limit, the second point is the concept of reaching the risk/reward threshold within the target tissue as a function of therapeutic configuration (i.e. dose, vector, route selection). Other IM injection AAV studies in myocardium have reported similar observations with target oversaturation[28, 29], suggesting that the risk/reward ratio becomes greater with increasing viral genome copy number beyond these biological limits. Analogous to this study, it is plausible to conclude that a lower dose of SC versus SS would have achieved the required level of efficacy (i.e. at least 4 fold) in the myocardium. This relationship is important and may vary between populations and disease conditions[30, 31]. In fact, one key molecular study has suggested that S100A1 has a bimodal therapeutic window in vivo whereby additional transduced protein can be detrimental to myocyte function[32]. This precise relationship for AAV mediated S100A1 overexpression was not elucidated in this study due to the limitations of a single dose/liquid jet route and similar chronic disease conditions, but could be detailed in future studies. Thus, establishing the pharmacodynamic therapeutic window at the cellular level as a function of the overall therapeutic strategy may be possible.

Another key aspect of this study was evaluating the immune risk profile within the cardiac (i.e. CD38 mediator) and off target liver tissues, whereby the concept of approaching a threshold of chronic adaptive immune responses can be quantified in terms of off target GC presence. It is well established that AAV mediated gene therapies can elicit deleterious immune responses with dose escalation due to collateral overexpression[30]. Excessive cardiac target and off target expression (e.g. in the liver and the reticuloendothelial system) increases the risk for adaptive responses. The off target expression is first most influenced by the initial pharmacokinetics of the delivery route via systemic exposure, then by the vector's tropism and intracellular trafficking following initial uptake. These risks can be mitigated with prudent dose selection as a function of both delivery route and AAV vector design. For example with the route held constant in this study, the SC exhibited a disproportionately higher level of undesired collateral liver exposure as compared with SS. The combination of both collateral organ and excess cardiac overexpression was likely correlated with the dramatic increase in the CD38 immune activation marker. Based on the results, it appears this level of overexpression in the liver was well tolerated. However, our translational point is that there may be a quantified threshold and these metrics should be considered.

Another point realized when circumventing the limitations of this single route/dose study, was the striking performance of scAAV over ssAAV. The advantageous design of scAAV allows it to bypass the rate limiting therapeutic conversion step of second strand synthesis, dramatically increasing expression, - including perhaps as shown here in collateral organ tissues. Therefore, it is very likely that a much lower dose of the SC vector might have provided the same benefits yet reduced overall immune risks. Corroborated by our finding, the ssAAV vector second strand synthesis is notably poor in the liver when compared to sc

AAV as found in previous controlled dose studies in rodents[24]. This is our best reasonable explanation for the disparity in explaining the difference between the SS and SC off target liver transfer in this study, although there could be many other causes that are beyond the scope of this study.

Concluding, the demand for increasing the transfer efficiency of various delivery methods to improve overall safety is ever increasing given that the risks for viral mediated transfer cannot be eliminated. Here we demonstrate by comparison with other published data[33,34] that the liquid jet methodology is more cardiac specific with a much more favorable qPCR transfer heart/liver ratio. In this study the specificity range was 250:1 for SS to 1:1 for SC, while reported percutaneous catheter infusion levels can reach very inefficient ratios as poor as 1:10,000[34,35]. With further technical development, liquid jet injection may become a clinically viable AAV delivery strategy for cardiac surgeons. Strikingly, 50-60% of the patient population is ineligible for AAV trials employing percutaneous catheter delivery due to preexisting AAV immunity[36]. Efficient gene transfer may be possible using liquid jet delivery in these patients, currently excluded from clinical trials. It is anticipated that extensive modifications (e.g. variable pressure settings corresponding to different tissue types/thickness) would be needed to adapt liquid jet into a more practical surgical delivery method. The future generation applicator could conceivably be implemented readily as adjunctive treatment performed minimally invasively or as an adjunct to cardiac surgical procedures.

Materials and Methods

Thirty male Sprague Dawley rats (Charles Rivers Laboratories, Inc.; Age 76±10 days) received humane care in compliance with the NIH and guidelines established by the Institutional Animal Care and Use Committee at Carolinas Medical Center. Each rat received a baseline echocardiograhy and MI and rats were divided into 3 separate groups (n=8 ea.): one saline control (SA) and 2 experimental groups receiving a single dose 1.2×10^{11} vg of one of two different vectors; ssAAV9.S100A1 (SS) and scAAV9.S100A1 (SC). Following 10 weeks, all rats were evaluated with echocardiography, Quantitative Polymerase Chain Reaction (qPCR) assays for AAV9.S100A1 genome copies (GC), and both overall therapeutic S100A1 and immune activating CD38[37] proteins via fluorescence quantification.

Echocardiography

All rats were subjected to baseline and follow up 10 week post myocardial infarction echocardiography by an experienced, blinded evaluator. Anesthesia was induced and maintained with 1-5% isofluorane in the supine position. A Visual Sonics Vevo5000 Echocardiography unit with a high frequency probe was used for acquisition. Optimal view parameter ranges were held consistent by a trained user, 1.7 – 2.2 cm depth, 15-20MHz frequency, 60-70% Gain. Long axis and M-mode views were obtained for each animal. 3 individual data sets were acquired and averaged for 1 overall score set reported for each animal.

Liquid Jet Gene Delivery Technical Description

Detailed technical development and settings were identified for a thoracotomy in a previous marker gene study[18]. Figure 1A depicts the concept of liquid jet injection applied to the epicardial surface following mini thoracotomy with optimized delivery parameters. These parameters were previously identified using a super speed camera (Zeiss International, Thornwood NY) at the University of Pennsylvania Complex Fluids Laboratory in conjunction with non-survival models. Jet fluid exit velocity, dispersion coefficients, and distance for the rodent were determined previously. A depiction of the rodent model application in shown in Figure 1B.

Infarct Model

A pulse oximeter, a Harvard Apparatus Ventilator, and an ECG monitor were used for surgery following induction with ketamine (4mg/kg IV) and intubation followed. Thereafter, mechanical ventilation was achieved for all rodents and then each was set in the left decubitus position sequentially prepared for a left mini-thoracotomy under aseptic conditions. Once the heart was exposed, the left anterior descending artery (LAD) was identified. The midline of the artery was marked with a surgical pen, and then 7.0 prolene sutures were used to ligate the artery. Infarct creation was confirmed by both myocardial discoloration and ECG changes (ST-segment depression) for each animal prior to delivery execution. Standard observations and post-operative care guidelines including pain management and fluid administration were administered.

Liquid Jet Mediated Delivery

Following infarction and a brief 15 minute monitoring period, each animal received 3 separate 100μL injections of either saline, SS AAV9.S100A1 or SC AAV9.S100A1 by Liquid Jet Injection. Total dose for the SS and SC was fixed at 1.2×10^{11} viral particles. The anterior, lateral, and posterior-lateral wall regions were injected by carefully aligning the jet per region. All animals were then recovered and monitored until 10 weeks. The heart was harvested, with myocardial cross sections and individual samples prepared for assay testing.

AAV Viral Vector Production

Both recombinant strains of ss and sc AAV.S100A1 were sourced from the University of Pennsylvania Vector Core (Philadelphia, PA). Specifically these were comprised of serotype-9 viral capsid and a single strand or double strand of encoded DNA: containing the S100A1 marker gene driven by a cytomegalovirus immediate-early promoter/enhancer, a hybrid intron, and a bovine growth hormone polyadenylation signal. Manufacturing process details of both strains can be found online (http://www.med.upenn.edu/gtp/vectorcore/). Following production, viral preps were pooled from individual lots and aliquoted in sterile vials each containing a dose of 2×10^{11} vp in 500μL volume.

qPCR Detection of Therapeutic AAV.S100A1 Genome Copies

All servicing was performed blinded by the Molecular Profiling Core at the Cannon Research Center. Three separate cardiac zones were harvested from each animal along the plane of injections: Anterior Wall, Borderzone i.e. (anterior to lateral wall region along

infarct), and the Lateral Wall. The liver was selected as the primary organ to quantify systemic exposure and was also collected for each animal. Briefly, whole DNA was isolated using the Chemagen MSM1 kit. Customized S100A1 primers human S100A1 (NM_006271.1, forward primer 5′-cgatggagaccctcatcaa-3, reverse primer 5′-tggaagtccacctccccgtc-3′) specific to only viral DNA were used. The level of rat GAPDH DNA was used to calculate normalized transfection with the ΔΔCt method to obtain qPCR values. Absolute genomic copies of S100A1 DNA were quantified with the standard normal curve built from serial dilutions. Data was reported as thousands of viral genome copies (GC) per 100 ng of whole DNA. Samples that were either reported error, zero undetectable or those >100,000 GC per 100 ng DNA were removed from the grouping analysis.

Immunofluorescence Staining of Protein: Therapeutic S100A1 and Immune Activator CD38

Briefly, all sample slides were subjected to heat induced antigen retrieval in citrate buffer (pH 6.0) and/or in proteinase. Slides were incubated for 1 hour/overnight with primary antibodies (CD38) Santa Cruz# sc-70654 and S100A1 Santa Cruz#sc-7849-R) after blocking with nonspecific antigenicity blocker. Corresponding fluorescent conjugated secondary antibodies were applied for 1 hour at room temperature. 4,6-Diamidino-2-phenylindole (DAPI) was included with the secondary antibodies to visualize nuclei. The staining, imaging and image analysis were performed by Cares Bio Laboratory, LLC (Shelton, CT, USA).

Confocal Microscopy & Image Quantification of S100A1/CD38 Levels

Briefly, cardiac section slides were scanned at Cares Bio Laboratory, LLC (Shelton, CT, USA) using a customized, computer-controlled microscope (Zeiss LSM780 confocal microscope, Carl Zeiss GMBh, Jena, Germany) with ×40 and ×20 objective. Every case had 32 image captures including 16 images per section. Images were analyzed using an image analysis software based on MATLAB (R2011b, Math Works), developed by Cares Bio Laboratory. A 32 array myocardial grid, featuring 8 random but separate zones defined in the anterior, lateral, posterior and septal wall regions were obtained for analysis at 20× magnification. Image analysis algorithms were applied to the images generated from microscopic slides of tissues stained with secondary antibody and isotype controls to generate the background score. A composite overall expression score consisting of the averaged individual cardiac zones normalized to control (i.e. 1.0 background endogenous S100A1/CD38) was computed for each animal.

Confocal Microscopy of Viral Mediated S100A1 Transduction

With the same microscopy suite, a series of ten random left ventricular ×20 objective images were capture for each animal and analyzed for % of cells expressing viral mediated S100A1. Positive threshold detection was normalized to a positive control (i.e. AAV.S100A1 from previous experiments) and applied for each image. One averaged score was reported for each animal, then for each group.

Infarct Size Characterization

Formalin fixed paraffin embedded LV cross sections were sectioned at 4 microns on a Leica RM2125. Slides were then baked in a 60 degree oven for 20 minutes to remove excess paraffin before being deparaffinized with xylene and rehydrated with several changes of graded alcohol to distilled water. H&E sections were stained with Mayer's hematoxylin for 20 minutes, rinsed with running tap water and stained with Eosin Y for 5 seconds followed by several rinses in 95% alcohol. Masson's Trichrome slides were stained with Weigert's Iron Hematoxylin for 10 minutes followed by a rinse in tap water. The rest of the staining was done with a Masson's Trichrome kit purchased from Polyscientific (Bay Shore, NY cat# k037). The slides were then dehydrated and coverslipped with Permount. Resultant images were then loaded into IMAGEJ software, whereby positive blue zones scored as infarct were represented as a % of overall LV cross sectional area to determine size. Two separate cross section runs were performed for each animal, with the highest score of the two being reported for each. Group scores were then averaged.

Statistical Analysis

All data are reported as mean ± standard error of the mean (SEM), per delivery group/data point. The Bartlett's test was used to verify equal variances within all measures. Single way ANOVA was used to determine difference across all 3 groups or for image capture analysis to ensure consistency. A post hoc Tukey's test was then used to determine comparative differences between groups at the 0.05 confidence level. Paired T-testing was used to determine differences for groups over time.

Acknowledgments

This study was graciously supported by the Heineman Foundation as well as NIH grant 2-R01 HL083078-08. We would also like to acknowledge the Gene Therapy Resource Program (GTRP) of the National Heart, Lung and Blood Institute for their gracious support in providing all AAV vectors necessary for this study, in particular Dr. Julie Johnston for custom analysis in the design phase. We also thank the Vivarium staff at Carolinas Medical Center for their outstanding effort with supporting the procedures and postoperative care and Dr. Sriparna Ghosh who performed all of the Confocal microscopy analysis.

This study received support from the Heineman Foundation, NIH grant 2-R01 HL083078-08, and the Gene Therapy Resource Program (GTRP) of the National Heart, Lung and Blood Institute.

References

1. Most P, Bernotat J, Ehlermann P, Pleger ST, Reppel M, Börries M, et al. S100A1: A regulator of cardiac contractility. Proc Natl Acad Sci USA. 2001; 98(24):13889–94. [PubMed: 11717446]
2. Most P, Remppis A, Pleger ST, Katus HA, Koch WJ. S100A1: A novel inotropic regulator of cardiac performance. Transition from molecular physiology to pathophysiological relevance. Am JP hysiol Regul Integr Comp Physiol. 2007; 293:R568–77.
3. Pleger ST, Most P, Boucher M, Soltys S, Chuprun JK, Pleger W, et al. Stable myocardial-specific AAV-S100A1 gene therapy results in chronic functional heart failure rescue. Circulation. 2007; 115:2506–15. [PubMed: 17470693]
4. Boerries M, Most P, Gledhill JR, Walker JE, Katus HA, Koch WJ, et al. Ca2+ -dependent interaction of S100A1 with F1-ATPase leads to an increased ATP content in cardiomyocytes. Mol Cell Biol. 2007; 27:4365–73. [PubMed: 17438143]

5. Yamasaki R, Berri M, Wu Y, Trombitás K, McNabb M, Kellermayer MS, et al. Titin-actin interaction in mouse myocardium: passive tension modulation and its regulation by calcium/S100A1. Biophys J. 2001; 81:2297–313. [PubMed: 11566799]
6. Maco B, Mandinova A, Durrenberger MB, Schafer BW, Uhrik B, Heizmann CW. Ultrastructural distribution of the S100A1 Ca2+-binding protein in the human heart. Physiol Res. 2001; 50:567–74. [PubMed: 11829317]
7. Most P, Remppis A, Pleger ST, Loffler E, Ehlermann P, Bernotat J, et al. Transgenic overexpression of the Ca2+ binding protein S100A1 in the heart leads to increased in vivo myocardial contractile performance. J Biol Chem. 2003; 5:33809–17. [PubMed: 12777394]
8. Most P, Seifert H, Gao E, Funakoshi H, Volkers M, Heierhorst J, et al. Cardiac S100A1 protein levels determine contractile performance and propensity toward heart failure after myocardial infarction. Circulation. 2006; 114:1258–68. [PubMed: 16952982]
9. Katz MG, Fargnoli AS, Williams RD, Bridges CR. The road ahead: working toward effective clinical translation of myocardial gene therapies. Ther Deliv. 2014; 5:39–51. [PubMed: 24341816]
10. Fargnoli AS, Katz MG, Yarnall C, Sumaroka MV, Stedman H, Rabinowitz JJ, et al. A pharmacokinetic analysis of molecular cardiac surgery with recirculation mediated delivery of βARKct gene therapy: developing a quantitative definition of the therapeutic window. J Card Fail. 2011; 17:691–9. [PubMed: 21807332]
11. Katz MG, Fargnoli AS, Bridges CR. Myocardial gene transfer: routes and devices for regulation of transgene expression by modulation of cellular permeability. Hum Gene Ther. 2013; 24:375–92. [PubMed: 23427834]
12. Katz MG, Swain JD, Tomasulo CE, Sumaroka M, Fargnoli AS, Bridges CR. Current Strategies for myocardial gene delivery. J Mol Cell Cardiol. 2011; 50:766–76. [PubMed: 20837022]
13. Katz MG, Fargnoli AS, Williams RD, Bridges CR. Gene therapy delivery systems for enhancing viral and nonviral vectors for cardiac diseases: current concepts and future applications. Hum Gene Ther. 2013; 24:914–27. [PubMed: 24164239]
14. Rosengart TK, Lee LY, Patel SR, Sanborn TA, Parikh M, Bergman GW, et al. Angiogenesis gene therapy: phase I assessment of direct intramyocardial administration of an adenovirus vector expressing VEGF121 cDNA to individuals with clinically significant severe coronary artery disease. Circulation. 1999; 100:468–74. [PubMed: 10430759]
15. Jaski BE, Jessup ML, Mancini DM, Cappola TP, Pauly DF, Greenberg B, et al. Calcium upregulation by percutaneous administration of gene therapy in cardiac disease (CUPID Trial), a first-in-human phase 1/2 clinical trial. J Card Fail. 2009; 15:171–81. [PubMed: 19327618]
16. Jessup M, Greenberg B, Mancini D, Cappola T, Pauly DF, Jaski B, et al. Calcium upregulation by percutaneous administration of gene therapy in cardiac disease (CUPID): a phase 2 trial of intracoronary gene therapy of sarcoplasmic reticulum Ca2+-ATPase in patients with advanced heart failure. Circulation. 2011; 124:304–13. [PubMed: 21709064]
17. Hajjar RJ, Zsebo K, Deckelbaum L, Thompson C, Rudy J, Yaroshinsky A, et al. Design of a phase 1/2 trial of intracoronary administration of AAV1/SERCA2a in patients with heart failure. J Card Fail. 2008; 14:355–67. [PubMed: 18514926]
18. Fargnoli AS, Katz MG, Williams RD, Margulies KB, Bridges CR. A needleless liquid jet injection delivery method for cardiac gene therapy: a comparative evaluation versus standard routes of delivery reveals enhanced therapeutic retention and cardiac specific gene expression. J Cardiovasc Transl Res. 2014; 7:756–67. [PubMed: 25315468]
19. McCarty DM, Fu H, Monahan PE, Toulson CE, Naik P, Samulski RJ. Adeno-associated virus terminal repeat mutant generates self-complementary vectors to overcome the rate-limiting step to transduction in vivo. Gene Ther. 2003; 10:2112–8. [PubMed: 14625565]
20. Ferrari FK, Samulski T, Shenk T, Samulski RJ. Second-strand synthesis is a rate limiting step for efficient transduction by recombinant adeno-associated virus vectors. J Virol. 1996; 70:3227–34. [PubMed: 8627803]
21. Fisher KJ, Gao GP, Weitzman MD, DeMatteo R, Burda JF, Wilson JM. Transduction with recombinant adeno-associated virus for gene therapy is limited by leading-strand synthesis. J Virol. 1996; 70:520–32. [PubMed: 8523565]

22. Wang J, Xie J, Lu H, Chen L, Hauck B, Samulski RJ, et al. Existence of transient functional double-stranded DNA intermediates during recombinant AAV transduction. Proc Natl Acad Sci USA. 2007; 104:13104–9. [PubMed: 17664425]
23. Koeberl DD, Pinto C, Sun B, Li S, Kozink DM, Benjamin DK Jr, et al. AAV vector-mediated reversal of hypoglycemia in canine and murine glycogen storage disease type Ia. Mol Ther. 2008; 16:665–72. [PubMed: 18362924]
24. Andino LM, Conlon TJ, Porvasnik SL, Boye SL, Hauswirth WW, Lewin AS. Rapid, widespread transduction of the murine myocardium using self-complementary adeno-associated virus. Genet Vaccines Ther. 2007; 5:13. [PubMed: 18070352]
25. Wu J, Zhao W, Zhong L, Han L, Li B, Ma W, et al. Self-complementary recombinant adeno-associated viral vectors: packaging capacity and the role of rep proteins in vector purity. Hum Gene Ther. 18:171–82. [PubMed: 17328683]
26. Most P, Raake P, Weber C, Katus HA, Pleger ST. S100A1 gene therapy in small and large animals. Methods Mol Biol. 2013; 963:407–20. [PubMed: 23296625]
27. Pleger ST, Shan C, Ksienzyk J, Bekeredjian R, Boekstegers P, Hinkel R, et al. Cardiac AAV9-S100A1 gene therapy rescues post-ischemic heart failure in a preclinical large animal model. Sci Transl Med. 2011; 3:92ra64.
28. Blankinship MJ, Gregorevic P, Allen JM, Harper SQ, Harper H, Halbert CL, et al. Efficient transduction of skeletal muscle using vectors based on adeno-associated virus serotype 6. Mol Ther. 2004; 10:671–8. [PubMed: 15451451]
29. Wang Z, Zhu T, Qiao C, Zhou L, Wang B, Zhang J, et al. Adeno-associated virus serotype 8 efficiently delivers genes to muscle and heart. Nat Biotechnol. 2005; 3:321–8. [PubMed: 15735640]
30. Mays LE, Wilson JM. The complex and evolving story of T cell activation to AAV vector-encoded transgene products. Mol Ther. 2011; 1:16–27. [PubMed: 21119617]
31. Pfeffer MA, Braunwald E. Ventricular remodeling after myocardial infarction. Experimental observations and clinical implications. Circulation. 1990; 81:1161–72. [PubMed: 2138525]
32. Weber C, Neacsu I, Krautz B, Schlegel P, Sauer S, Raake P, et al. Therapeutic safety of high myocardial expression levels of the molecular inotrope S100A1 in a preclinical heart failure model. Gene Ther. 2014; 21:131–8. [PubMed: 24305416]
33. Byrne MJ, Power JM, Preovolos A, Mariani JA, Hajjar RJ, Kaye DM. Recirculating cardiac delivery of AAV2/1SERCA2a improves myocardial function in an experimental model of heart failure in large animals. Gene Ther. 2008; 15(23):1550–7. [PubMed: 18650850]
34. Kaye DM, Preovolos A, Marshall T, Byrne M, Hoshijima M, Hajjar R, et al. Percutaneous cardiac recirculation-mediated gene transfer of an inhibitory phospholamban peptide reverses advanced heart failure in large animals. J Am Coll Cardiol. 2007; 50:253–60. [PubMed: 17631218]
35. Bridges CR. 'Recirculating cardiac delivery' method of gene delivery should be called non-recirculating method. Gene Ther. 2009; 16:939–40. [PubMed: 19340020]
36. Liu Q, Huang W, Zhang H, Wang Y, Zhao J, Song A, et al. Neutralizing antibodies against AAV2, AAV5 and AAV8 in healthy and HIV-1-infected subjects in China: implications for gene therapy using AAV vectors. Gene Ther. 2014; 21:732–8. [PubMed: 24849042]
37. Partidá-Sánchez S, Rivero-Nava L, Shi G, Lund FE. CD38: an ecto-enzyme at the crossroads of innate and adaptive immune responses. Adv Exp Med Biol. 2007; 590:171–83. [PubMed: 17191385]

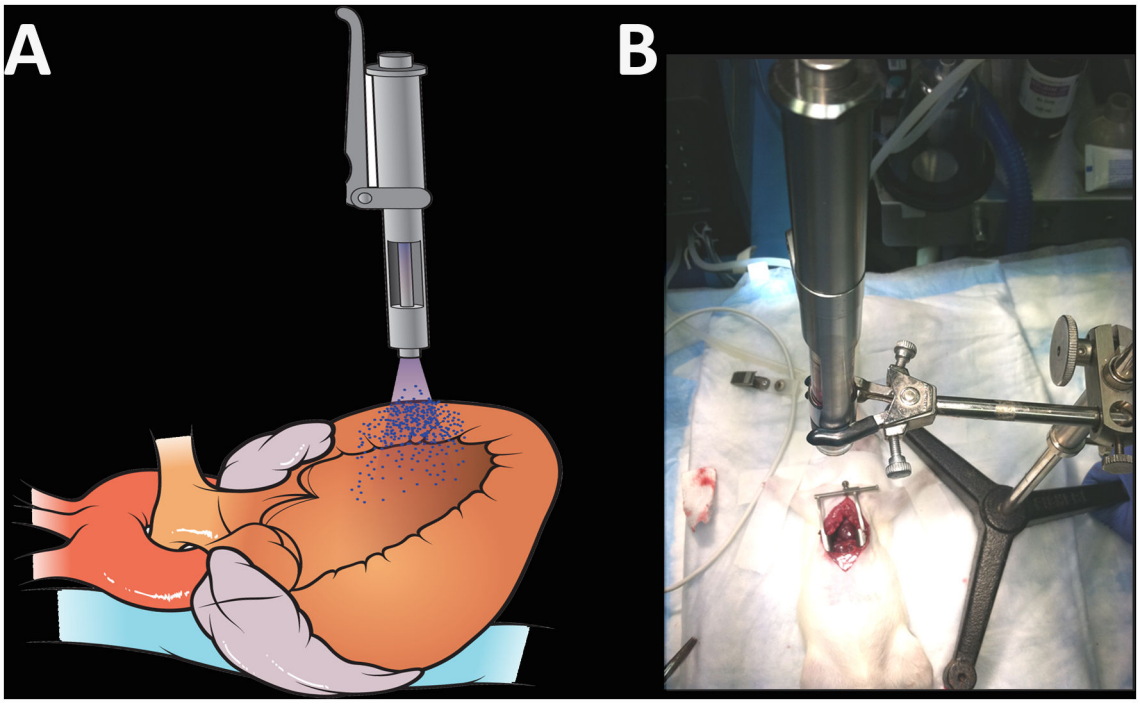

Figure 1.

A. The concept of liquid jet injection for cardiac gene therapy. A high pressurized jet of therapeutic is projected toward the epicardial surface of beating myocardium through a minimally invasive thoracotomy or as an adjunctive cardiac surgical procedure. Myocardial retention within safety limits can be optimized via parameter adjustment.

B. The liquid jet delivery concept applied to the rodent model. The DERMOJet injector device mounted to a control arm for guidance of precise injections to the beating heart.

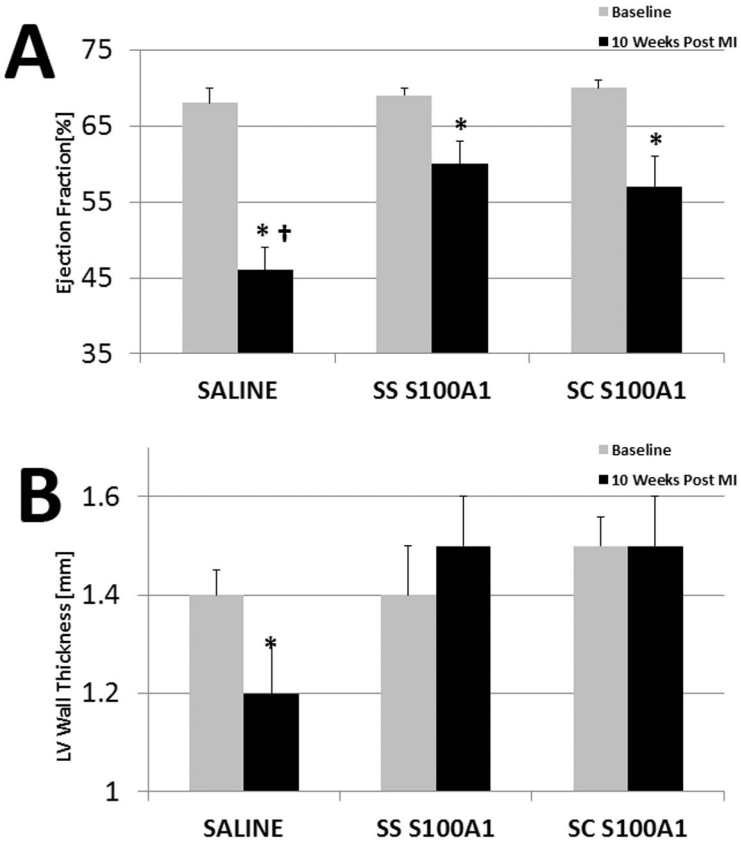

Figure 2.

A. Gene therapy treatment groups demonstrate superior left ventricular performance via Ejection Fraction compared with saline and preserve more baseline function, * $p<0.05$, Baseline vs. 10 Week MI time point by group; † $p<0.05$, Saline Control group vs. both S100A1 groups at 10 Weeks Post MI.

B. Gene therapy treatment groups demonstrate preserved left ventricular geometry via retained global LV wall thickness compared with Saline Control which deteriorated significantly from baseline, * $p<0.05$, Baseline vs. 10 Week MI time point by group.

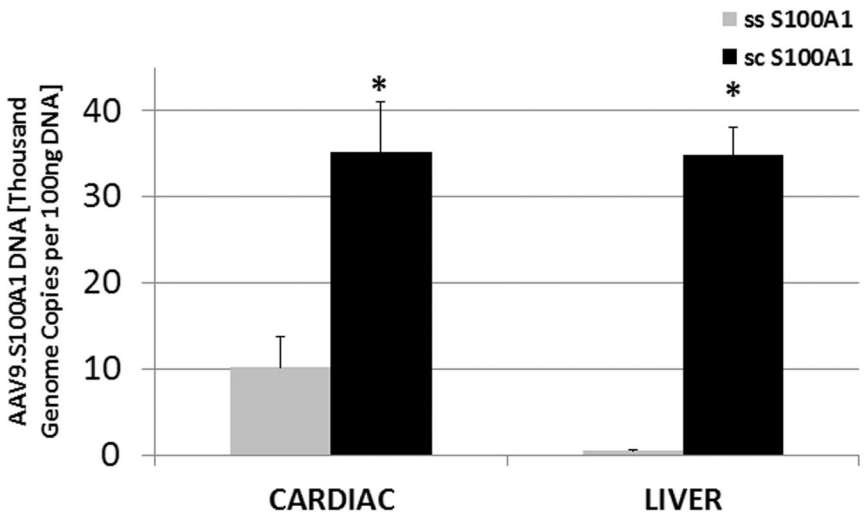

Figure 3.

Quantitative Poly Chain Reaction (QPCR) derived quantification of viral mediated S100A1 DNA. The SC vector performed significantly greater than the SS with much higher genome copies detected in both target cardiac and collateral liver organ tissues, * $p<0.05$.

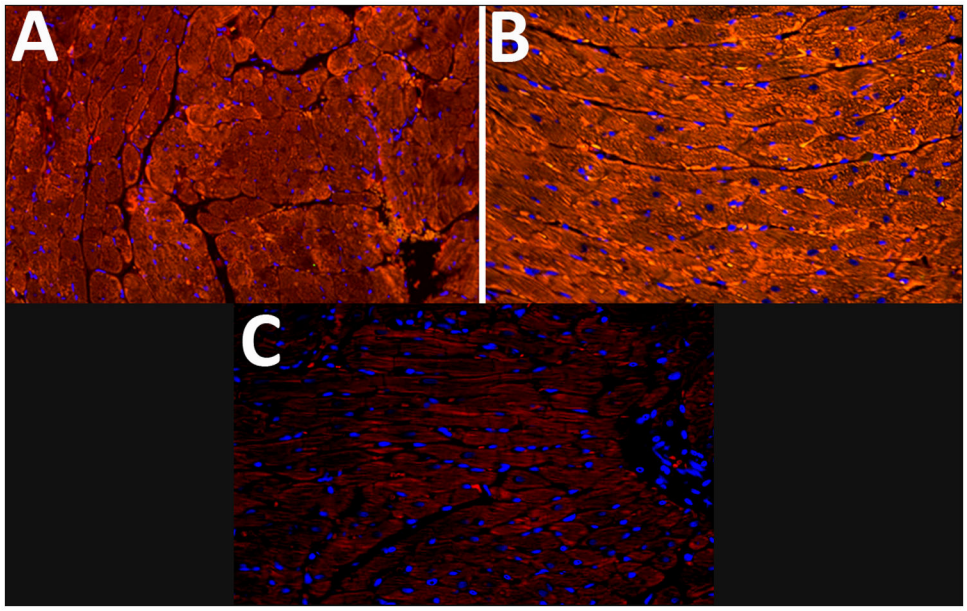

Figure 4.

A. Confocal microscopy image capture of typical myocardium with overexpression of S100A1 (orange-brown) featuring homogenous robust profile from the liquid jet injection methodology in the SS group, magnification 20×.

B. A greater degree of S100A1 (orange-brown) overexpression featuring was confirmed in the SC group specimens, magnification 20×.

C. Confocal microscopy image capture of typical myocardium with overexpression of S100A1 (orange-brown) featuring control level profile from the liquid jet injection methodology in the SA group, magnification 20×.

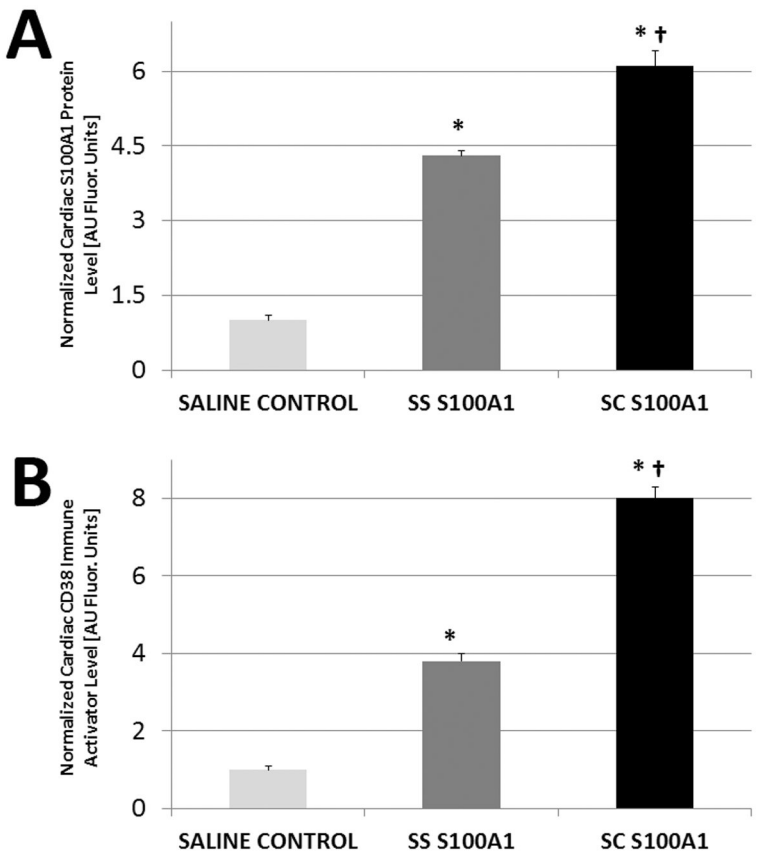

Figure 5.

A. Quantitative immunofluorescence of therapeutic S100A1 protein demonstrates significantly higher target levels in both the SS and SC groups vs. Saline Control.* $p<0.05$, SS and SC groups vs. Saline Control; † $p<0.05$, SC vs. SS.

B. Quantitative immunofluorescence of immune activator risk factor CD38 protein demonstrates significantly higher cardiac tissue levels in the SS and SC groups Saline vs. Control.* $p<0.05$, SS and SC groups vs. Saline Control; † $p<0.05$, SC vs. SS.

Table 1

Echocardiography & Outcome Data

	Baseline		
Data Point:	**Saline**	**ssAAV S100A1**	**scAAV S100A1**
Weight [g]	406±32	382±13	336±24
Heart Rate [bpm]	346±9	339±9	318±13
End Diastoic Volume Index [mL/cm^2]	0.71±0.1	0.62±0.1	0.76±0.04
End Systolic Volume Index [mL/cm^2]	0.24±0.05	0.19±0.03	0.23±0.02
Stroke Volume Index [mL/cm2]	0.48±0.06	0.43±0.06	0.53±0.04
Ejection Fraction [%]	68±2	69±1	70±1
Epicardial 2D Area [cm^2]	0.8±0.1	0.7±0.1	0.8±0.1
LV Wall Thickness [mm]	1.4±0.05	1.4±0.1	1.5±0.06
	10 Weeks Post MI		
Data Point:	Saline	**ssAAV S100A1**	**scAAV S100A1**
Weight [g]	610±22 *	568±21 *	573±8 *
Heart Rate [bpm]	317±9 *	286±11 *	309±13
End Diastoic Volume Index [mL/cm^2]	1.33±0.1 *	1.22±0.2 *	1.33±0.2 *
End Systolic Volume Index [mL/cm^2]	0.73±0.1 *	0.49±0.1 *	0.57±0.2 *
Stroke Volume Index [mL/cm2]	0.61±0.1 *	0.73±0.1 *,†	0.76±0.1 *,†
Ejection Fraction [%]	46±3 *	60±3 *,†	57±4 *,†
Epicardial 2D Area [cm^2]	1.5±0.1 *	1.4±0.1 *	1.5±0.1 *
LV Wall Thickness [mm]	1.2±0.1 *	1.5±0.1	1.5±0.1
Δ Stroke Volume Index [mL/cm^2]$_{10\ Weeks\ -\ Baseline}$	0.10±0.03	0.30±0.04 †	0.25±0.05 †
Infarct Size [% LV Area]$_{10\ Weeks}$	29±4	25±4	37±6

* p<0.05; Baseline to 10 Weeks

† p <0.01; vs. Saline Control Group